JACS
JOURNAL OF THE AMERICAN CHEMICAL SOCIETY

COMMUNICATION

pubs.acs.org/JACS

Self-Assembled Peptide Architecture with a Tooth Shape: Folding into Shape

Sunbum Kwon,[†] Hye Sun Shin,[‡] Jintaek Gong,[†] Jae-Hoon Eom,[†] Aram Jeon,[†] Sung Hyun Yoo,[†] Im Sik Chung,[§] Sung June Cho,[*,‡] and Hee-Seung Lee[*,†]

[†]Molecular-Level Interface Research Center, Department of Chemistry, KAIST, Daejeon 305-701, Korea

[‡]Department of Applied Chemical Enginnering, Chonnam National University, Gwangju 500-757, Korea

[§]BioNanotechnology Research Center, Korea Research Institute of Bioscience and Biotechnology, Daejeon 305-333, Korea

Supporting Information

ABSTRACT: Molecular self-assembly is the spontaneous association of molecules into structured aggregates by which nature builds complex functional systems. While numerous examples have focused on 2D self-assembly to understand the underlying mechanism and mimic this process to create artificial nano- and microstructures, limited progress has been made toward 3D self-assembly on the molecular level. Here we show that a helical β-peptide foldamer, an artificial protein fragment, with well-defined secondary structure self-assembles to form an unprecedented 3D molecular architecture with a molar tooth shape in a controlled manner in aqueous solution. Powder X-ray diffraction analysis, combined with global optimization and Rietveld refinement, allowed us to propose its molecular arrangement. We found that four individual left-handed helical monomers constitute a right-handed superhelix in a unit cell of the assembly, similar to that found in the supercoiled structure of collagen.

Regardless of scales and constituents, object shape is a subject of fundamental interest for scientists in various fields. In most cases, shapes in biological systems are constructed through precisely controlled self-assembly based on blueprints that are not fully understood.[1] In the past, tremendous effort has been devoted to mimicking self-assembly.[2−6] However, control of three-dimensional (3D) self-assemblies in a laboratory setting remains far behind that of natural systems in terms of diversity, periodicity, and size and shape homogeneities. These challenges are partially due to the difficulty in the design and use of nondirectional noncovalent interactions, such as van der Waals and hydrophobic interactions, in synthetic, nonbiological systems.[7,8] The self-assembly of peptide-based molecular systems is especially complex and difficult to control because of their intrinsic conformational flexibility and diverse side-chain functionality.[9] Thus, we sought to establish a set of self-assembling components that can be linked to observable 3D shapes by which the governing parameters of self-assembly can be disentangled and tractable. In this context, β-peptide foldamers (oligomers of β-amino acids) are excellent candidates for a model system that meets these minimum requirements of rigidity and predictability because, in solution, they adopt rigid and controllable secondary structures.[10−14]

We and others have recently examined the self-associating behavior of β-peptides.[15−18] Our group previously discovered that a β-peptide with a specific folding propensity self-assembles in aqueous solution to form 3D molecular architectures with unprecedented shapes.[18] This unusual 3D shape formation is attributed to the unique conformational features of the building block. This study has encouraged us to devise a new term, "foldectures" (a compound of "foldamer" and "architectures"), to describe any 3D molecular architecture that is derived from the self-association of foldamers in solution. The ability to relate the secondary structures of foldamers to their 3D shapes will clarify the interactions that underlie molecular recognition and self-assembly, and help rationalize the macroscopic properties of organic materials in terms of their microscopic molecular structures. The concept of "folding into architectures or shapes" can be expanded to the study of the fundamental links between constituents and shapes on multiple scales by using systematic experimental and theoretical methods. Herein, we report a new foldecture that exhibits a molar tooth shape and is formed by the controlled self-assembly of a short helical β-peptide. Assembly analyses using synchrotron powder X-ray diffraction (PXRD), combined with global optimization and refinement, allowed us to obtain new insight into its detailed molecular arrangement.

In our self-assembly studies, we opted to use a homo-oligomer of *trans*-(*R*,*R*)-2-aminocyclopentanecarboxylic acid (*trans*-(*R*,*R*)-ACPC) as a building block. As shown in its molecular structure (Scheme 1a), the ACPC hexamer ($ACPC_6$) is an oligomer that consists of six *trans*-(*R*,*R*)-ACPC monomers in which the N- and C-termini are protected by *tert*-butyloxycarbonyl (Boc) and benzyl groups, respectively.[13] $ACPC_6$ adopts a stable left-handed 12-helix via intramolecular hydrogen bonding between C═O (*i*) and N−H (*i*+3) in solution (Supporting Information (SI) Figure S1). We performed the self-assembly study in the presence of a nonionic surfactant, Pluronic P123 (a triblock copolymer). A solution of $ACPC_6$ in THF (50 μL, 2 mg mL^{-1}) was added to an aqueous solution of P123 (2 mL, 8 g L^{-1}) with vigorous stirring for 1 min at 0 °C. The resulting solution was then aged for 3 h at 20 °C (ambient temperature), during which a white precipitate gradually separated from the solution.

Scanning electron microscopy (SEM) analyses of the filtered material revealed a very intriguing morphology, M_P, as presented in Figure 1a. The unique shape of the self-assembly resembles a molar tooth in which the upper half of the shape appears to be a

Received: September 1, 2011
Published: October 10, 2011

dx.doi.org/10.1021/ja2082476 | *J. Am. Chem. Soc.* 2011, 133, 17618–17621

Scheme 1. (a) Chemical Structure and Molecular Model of *trans*-(*R*,*R*)-ACPC$_6$ and (b) Schematic Representation of This Work

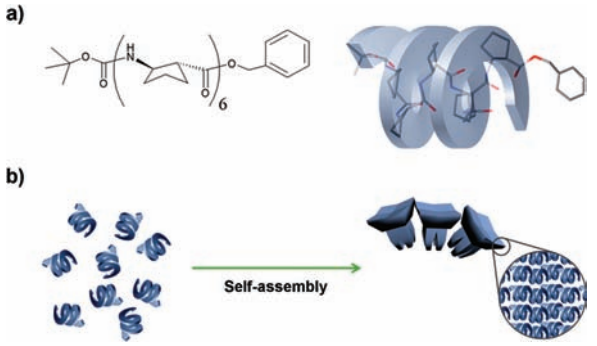

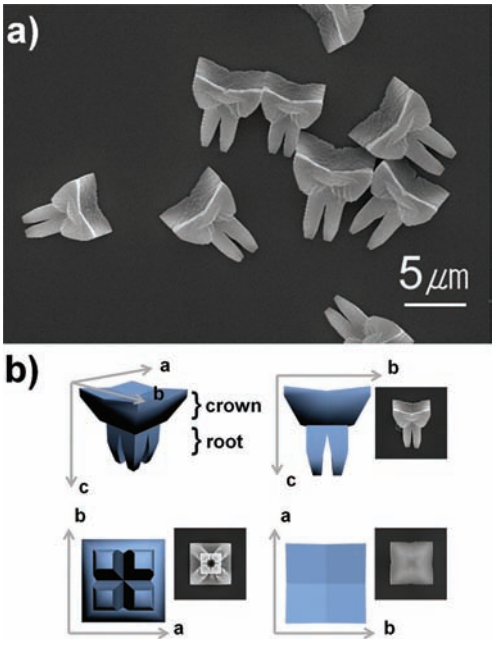

Figure 1. (a) SEM image of the molar tooth-shaped self-assembled structure of ACPC$_6$ (M_P). (b) 3D schematic representation of M_P in which the arbitrary axes *a*, *b*, and *c* are orthogonal to one another (top left). Schematic representations with their corresponding SEM images, as viewed from the *a* axis (top right), *c*(+) axis (bottom left), or *c*(−) axis (bottom right) are depicted.

blunt crown and the lower half resembles a root-like structure (Figure 1b, top left). These structures also have fairly good shape and size homogeneity (ca. 5 μm × 5 μm × 6 μm). When viewed perpendicular to the *ab* plane, it displays four roots, and the 2D shape exhibits a unique pattern of alternating squares and crosses with C_{4v} symmetry (Figure 1b, bottom left). By contrast, the upside-down face is square-shaped and symmetrically deflected inward (Figure 1b, bottom right). To the best of our knowledge, such an amazingly well-defined, anisotropic 3D organic nanostructure has never been achieved via peptide self-assembly.

To investigate the role of P123 additive in the unique 3D shape formation, ACPC$_6$ self-assembly was performed at different experimental conditions and monitored by SEM (Figure 2a−c). When both stirring and aging processes were carried out at 0 °C, which is below the critical micellization temperature (CMT) of the aqueous solution of P123,[19] a square plate shape, X_P, was observed (Figure 2a). X_P displays flat 2D structure with a four-fold dendritic skeleton on its face. As shown in Figure 2b, however, the removed root part again appeared when the initially agitated mixture was aged for 30 min at elevated temperature, i.e., 20 °C (>CMT). The length of the root was fully restored to form a molar tooth shape with longer aging time at 20 °C (Figure 2c). These data clearly show that the root-part growth in the *c*-direction predominantly occurs during aging >CMT. These experimental results also imply that ACPC$_6$ preferentially assembles in the *ab* plane in the absence of P123 micelles; however, unidirectional assembly in the *c* direction was guided by the micellar form of P123.

From the stepwise temperature control experiments, it was found that micelle formation of P123 was crucial for the formation of the unique 3D shape.[18] The overall structure evolution process of molar tooth-shaped self-assembly is illustrated in Figure 2d. Since the effective micellization of P123 was not feasible at a temperature <CMT, the P123 additive could not induce *c*-directional growth. This hypothesis was also confirmed by a control experiment in which a similar shape (X_W) was obtained when self-assembly was performed in pure water (SI Figure S3). At 20 °C, which is above the CMT, P123 micelles recognize the functional anisotropy of the growing crystal at an early stage of the self-assembly process and selectively suppress the growth rate in the *a* and *b* directions, thereby rapidly increasing the growth rate in the *c* direction to form M_P.[20] Notably, we observed striking differences in the morphological features of the self-assemblies of the analogous β-peptide building blocks, ACPC$_6$ and ACPC$_7$. Although these structures adopted the same 12-helix, a single-residue deletion was sufficient for inducing dramatic morphological changes on the level of the self-assembled structure.

The PXRD data showed that the two relevant shapes (M_P and X_P) had almost identical, well-defined diffraction patterns, suggesting that these assemblies share similar molecular packing structures (SI Figure S7). To unravel this molecular packing structure, high-resolution synchrotron XRD was performed, and the molar shape foldecture M_P was sampled under ambient conditions at the Pohang Accelerator Laboratory. The resulting diffraction patterns were indexed using DICVOL06.[21] The resulting lattice parameters for the foldecture (M_P) unit cell were as follows: a = 10.481 Å, b = 10.481 Å, c = 44.546 Å, α = 90.0°, β = 90.0°, and γ = 90.0°. The foldecture was also found to have tetragonal symmetry with a high figure of merit (FOM (20), 210.4). Interestingly, these parameters were completely different than those of the single ACPC$_6$ crystal (i.e., triclinic with a = 8.6599 Å, b = 11.6888 Å, c = 12.9173 Å, α = 69.207°, β = 81.630°, and γ = 88.666°).[13]

Noteworthy, the resulting unit cell volume (4888 Å^3) was 4 times larger than that of the single crystal (1209 Å^3). Thus, four ACPC$_6$ molecules exist in a self-assembled unit cell.

The possible space groups were found to be $P4_1$, $P4_3$, $P4_122$, $P4_322$, $P4_12_12$, and $P4_32_12$, respectively.[22] Two space groups, $P4_1$ and $P4_3$, were enantiomorphously related (i.e., an enantiomorphic pair). The corresponding higher space groups were also enantiomorphously related.[23]

To obtain the initial ACPC$_6$ structure in the unit cell, global optimization was performed over the ACPC$_6$ structure using parallel tempering with a resolution (d) of 2.0 Å.[24] Initially, the single-crystal structure was assumed to be a rigid body. Before the optimization, Le Bail fitting (structureless parameter fitting) was performed to find the optimized profile parameters.[25] At this

dx.doi.org/10.1021/ja2082476 |*J. Am. Chem. Soc.* 2011, 133, 17618–17621

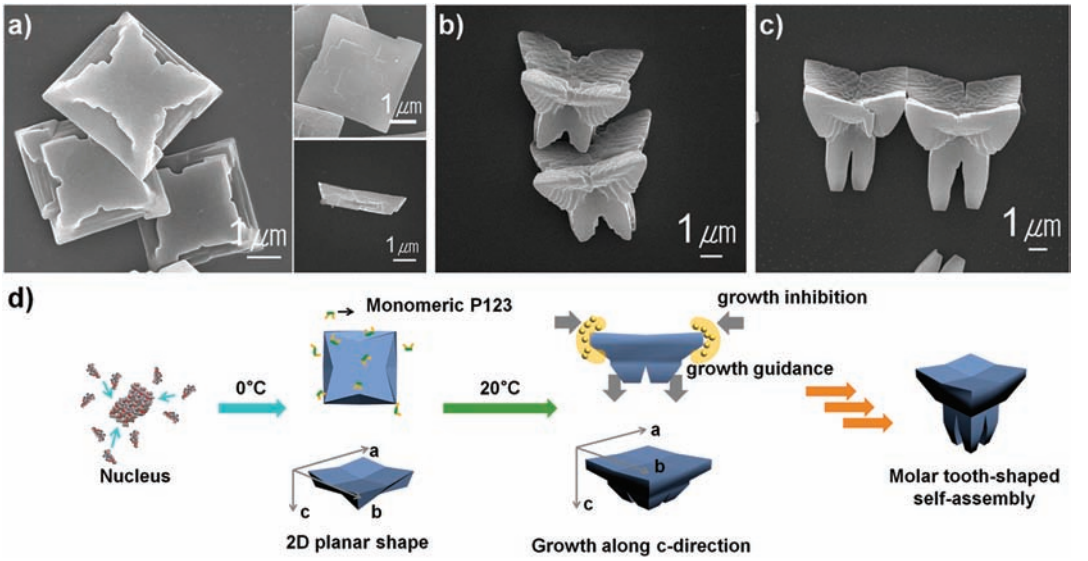

Figure 2. SEM images of self-assembled structures (a) obtained from 8 g L^{-1} of P123 aqueous solution at 0 °C (X_P) (inset: upside-down view, side view), (b) obtained from solution initially agitated at 0 °C for 1 min and aged at 20 °C for 30 min, and (c) obtained from solution initially agitated at 0 °C for 1 min and aged at 20 °C for 3 h. (d) Overall structure evolution process of molar tooth-shaped self-assembly.

stage, the result of the Le Bail fitting suggested that the lowest R_{wp} (7.25%) could be obtained using the $P4_1$ space group (SI Figure S8). The rigid-body structure was then optimized using parallel tempering without sacrificing the detailed structure; the number of trial runs was >2 000 000. The resulting structure was then considered to be a flexible model with automatic constraints and fully optimized to achieve a stable structure. During this process, the optimized structure was visually examined to see the overlap of the chains and atoms. This procedure was repeated more than 20 times for each space group. These complex procedures suggested that the only the $P4_1$ space group provides a non-overlapping, stable, optimized structure with the lowest R_{wp} and R_p values (16.7% and 12.8%, respectively), based on d = 2.0 Å. Thus, this structure was used as the initial structure for further Rietveld refinement.

For the Rietveld refinement, soft constraints were set for the $ACPC_6$ unit.[26] All of the bond distances (i.e., C−C, C−N, and C−O) and angles were initially restrained with a weight of 100 (SI Table S1). The weight was progressively decreased to 10 in the final refinement. The thermal displacement factor was set to the same value for atoms in identical functional groups, such as terminal CH_3, cyclopentane, and benzene. This restraint was maintained in the final refinement. SI Figure S9 shows the final Rietveld refinement results.[27] Up to d = 1.8 Å, the refinement was performed to provide reasonable fitting quality with the following data: R_{wp} = 7.65%, R_p = 5.46%, and R_F = 8.24%, respectively. The detailed structural parameters are listed in SI Table S2. Hydrogen atoms were geometrically added to the refined $ACPC_6$ structure (SI Figure S10).[28] The final refined structure was then superimposed onto the initial structure. The backbones of the two structures are in good agreement, but variation in the individual cyclopentane ring conformations was observed (SI Figure S11b).

Figure 3a illustrates the molecular structure of the M_P foldecture unit cell based on PXRD analysis. Four $ACPC_6$ monomers in the asymmetric unit formed a supercoiled helical structure in the c direction, while each $ACPC_6$ molecule adopted the characteristic 12-helix (left-handed). This formed a higher-order superhelix

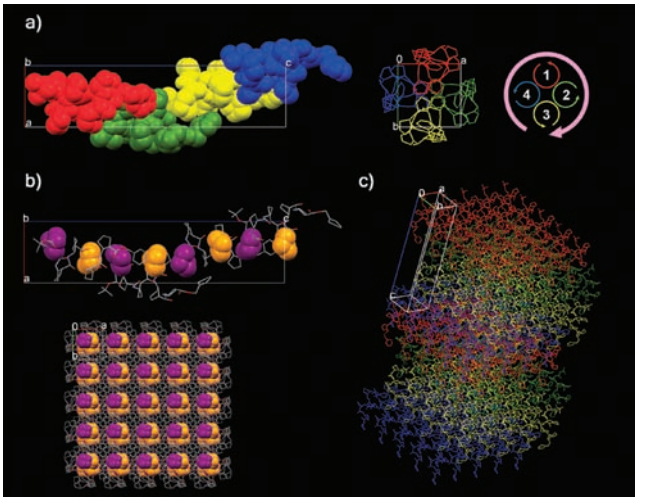

Figure 3. (a) Molecular structure of foldecture M_P in the unit cell. A space-filling model from a view perpendicular to the helix axis (left, N-terminus, left side) is shown. The individual $ACPC_6$ molecules in the unit cell are shown in red, green, yellow, and blue. A stick model from a view along the helix axis (middle) is also displayed. The helical handedness of the individual $ACPC_6$ molecules and that of the superhelix (pink) are shown (right). (b) Stick model from a view perpendicular to the helix axis (top, N-terminus, left side). A molecular network from a view along the c-axis (bottom) is also represented. The first (purple) and fourth (orange) cyclopentane rings of $ACPC_6$ are highlighted in the space-filling model. (c) A molecular network from a view along an arbitrary axis.

(right-handed), similar to that found in the supercoiled structure of collagen.[29] The helical pitch of the superhelix was 44.536 Å, which is almost identical to that of the unit cell parameter, c (44.546 Å). The superhelix axis was nearly parallel to the helix axis of the individual $ACPC_6$. A $(C{=}O)_{i+4}{\cdots}(H{-}N)_j$ intermolecular hydrogen bond was observed between two consecutive $ACPC_6$ units in the c direction. In addition, the cyclopentane ring of the fourth (shown in orange) and first hexamer ACPC residue

dx.doi.org/10.1021/ja2082476 |J. Am. Chem. Soc. 2011, 133, 17618–17621

(shown in purple) were stacked on top of one another in the interior of the superhelix, winding along the superhelix axis (Figure 3b). The other four ACPC residues of each $ACPC_6$ were located above the superhelical faces, which were responsible for lateral interactions through $(C{=}O)_{i+5}{\cdots}(H{-}N)_{j+1}$ hydrogen bonds and van der Waals contact. Figure 3c shows the molecular networks that were constructed on the basis of these intermolecular interactions. Interestingly, when viewed from the *c*-axis, the packing pattern exhibited a square shape with C_{4v} symmetry (Figure 3b, bottom), which seems to be related to its 2D shape when viewed perpendicular to the *ab* plane (Figure 1b, bottom left). Although the characteristic secondary structure (12-helix) of the monomeric unit in the self-assembled structure was almost identical to the corresponding single-crystal structure, the molecular packing pattern of the self-assembly was completely different from that of the crystal.

In summary, we have discovered a novel 3D molecular architecture that resembles a molar tooth and is formed via the controlled self-assembly of a short helical β-peptide. The unrivaled size uniformity and unique shape of this foldecture are attributed to the conformational rigidity of the monomeric unit in solution. This work also demonstrates how one can use nondirectional noncovalent interactions by design. The strategy of including large complementary molecular surfaces in the assembling unit served as the basis for molecular recognition in the self-assembly. A systematic study of the relationship between foldamers and their resulting 3D foldecture shapes, combined with the structural determination of molecular packing, will provide us with a comprehensive understanding of the self-assembly of natural components and the formation of sophisticated organic crystals.[30,31] In addition, the ability to spontaneously form 3D shapes using a bottom-up approach that is akin to biological assembly will simplify the preparation of optically active organic solids.

■ ASSOCIATED CONTENT

Supporting Information. Experimental procedures, additional figures, and characterizations. This material is available free of charge via the Internet at http://pubs.acs.org.

■ AUTHOR INFORMATION

Corresponding Author
hee-seung_lee@kaist.ac.kr; sjcho@chonnam.ac.kr

■ ACKNOWLEDGMENT

This research was supported by Basic Science Research Program through the National Research Foundation of Korea (NRF) grant funded by the Ministry of Education, Science and Technology (2009-0084449, 2011-0001318), and a grant from KRIBB Research Initiative Program.

■ REFERENCES

(1) Whitesides, G. M.; Mathias, J. P.; Seto, C. T. *Science* **1991**, *254*, 1312–1319.
(2) Yamamoto, Y.; Fukushima, T.; Suna, Y.; Ishii, N.; Saeki, A.; Seki, S.; Tagawa, S.; Taniguchi, M.; Kawai, T.; Aida, T. *Science* **2006**, *314*, 1761–1764.
(3) Ghadiri, M. R.; Granja, J. R.; Milligan, R. A.; McRee, D. E.; Khazanovich, N. *Nature* **1993**, *366*, 324–327.
(4) Reches, M.; Gazit, E. *Science* **2003**, *300*, 625–627.
(5) Hartgerink, J. D.; Beniash, E.; Stupp, S. I. *Science* **2001**, *294*, 1684–1688.
(6) Zhang, S. *Nat. Biotechnol.* **2003**, *21*, 1171–1178.
(7) Ulman, A. *Chem. Rev.* **1996**, *96*, 1533–1554.
(8) Bowden, N.; Terfort, A.; Carbeck, J.; Whitesides, G. M. *Science* **1997**, *276*, 233–235.
(9) Mayor, U.; Guydosh, N. R.; Johnson, C. M.; Grossmann, J. G.; Sato, S.; Jas, G. S.; Freund, S. M. V.; Alonso, D. O. V.; Daggett, V.; Fersht, A. R. *Nature* **2003**, *421*, 863–867.
(10) Gellman, S. H. *Acc. Chem. Res.* **1998**, *31*, 173–180.
(11) Appella, D. H.; Christianson, L. A.; Klein, D. A.; Powell, D. R.; Huang, X.; Barchi, J. J.; Gellman, S. H. *Nature* **1997**, *387*, 381–384.
(12) Porter, E. A.; Wang, X.; Lee, H. −S.; Weisblum, B.; Gellman, S. H. *Nature* **2000**, *404*, 565.
(13) Appella, D. H.; Christianson, L. A.; Klein, D. A.; Richards, M. R.; Powell, D. R.; Gellman, S. H. *J. Am. Chem. Soc.* **1999**, *121*, 7574–7581.
(14) *Foldamers: Structure, Properties, and Applications*; Hecht, S., Huc, I., Eds.; Wiley-VCH: Weinheim, Germany, 2007.
(15) Daniels, D. S.; Petersson, J.; Qiu, J. X.; Schepartz, A. *J. Am. Chem. Soc.* **2007**, *129*, 1532–1533.
(16) Martinek, T. A.; Hetényi, A.; Fülöp, L.; Mándity, I. M.; Tóth, G. K.; Dékány, I.; Fülöp, F. *Angew. Chem., Int. Ed.* **2006**, *45*, 2396–2400.
(17) Pizzey, C. L.; Pomerantz, W. C.; Sung, B.-J.; Yuwono, V. M.; Gellman, S. H.; Hartgerink, J. D.; Yethiraj, A.; Abbott, N. L. *J. Chem. Phys.* **2008**, *129*, 095103.
(18) Kwon, S.; Jeon, A.; Yoo, S. H.; Chung, I. S.; Lee, H. -S. *Angew. Chem., Int. Ed.* **2010**, *49*, 8232–8236.
(19) Alexandridis, P.; Holzwarth, J. F.; Hatton, T. A. *Macromolecules* **1994**, *27*, 2414–2415.
(20) Zhang, X.; Dong, C.; Zapein, J. A.; Ismathullakhan, S.; Kang, Z.; Jie, J.; Zhang, X.; Chang, J. C.; Lee, C.-S.; Lee, S.-T. *Angew. Chem., Int. Ed.* **2009**, *48*, 9121–9123.
(21) Boultif, A.; Louër, D. *J. Appl. Crystallogr.* **2004**, *37*, 724–731.
(22) *The CRYSFIRE 2002 System for Automatic Powder Indexing: User's Manual*; Shirley, R., Ed.; The Lattice Press: Guilford, Surrey, England, 2002.
(23) Palistrant, A. F. *Crystallogr. Rep.* **2009**, *54*, 539–547.
(24) Favre-Nicolin, V.; Černý, R. *J. Appl. Crystallogr.* **2002**, *35*, 734–743.
(25) Le Bail, A.; Duroy, H.; Fourquet, J. L. *Mater. Res. Bull.* **1988**, *23*, 447–452.
(26) McCusker, L. B.; Baerlocher, C. *Chem. Commun.* **2009**, 1439–1451.
(27) Larson, A. C.; Von Dreele, R. B. *General Structure Analysis System (GSAS) Los Alamos National Laboraoty Report LAUR* **2004**, *86*, 748.
(28) Cooper, R. I.; Thompson, A. L.; Watkin, D. J. *J. Appl. Crystallogr.* **2010**, *43*, 1100–1107.
(29) Bella, J.; Eaton, M.; Brodsky, B.; Berman, H. M. *Science* **1994**, *266*, 75–81.
(30) Horn, D.; Rieger, J. *Angew. Chem., Int. Ed.* **2001**, *40*, 4330–4361.
(31) Desiraju, G. R. *Nat. Mater.* **2002**, *1*, 77–79.